

## Supporting Information

### **Bioadhesive giant vesicles for monitoring hydroperoxidation in lipid membranes**

P. H. B. Aoki<sup>1,2,3</sup>, A. P. Schroder<sup>1</sup>, C. J. L. Constantino<sup>2</sup> and C. M. Marques<sup>1</sup>

<sup>1</sup>Institut Charles Sadron, Université de Strasbourg,  
CNRS UP 22, F-67034 Strasbourg Cedex 2, France.

<sup>2</sup>Faculdade de Ciências e Tecnologia, UNESP Universidade Estadual Paulista,  
Presidente Prudente, SP, 19060-900, Brazil

<sup>3</sup>São Carlos Institute of Physics, University of São Paulo,  
CP 369, 13560-970 São Carlos, SP, Brazil

## Materials

All phospholipids were purchased from Avanti Polar Lipids: 1-palmitoyl-2-oleoyl-sn-glycero-3-phosphocholine (POPC), 2-dioleoyl-sn-glycero-3-phosphocholine (DOPC), 1,2-distearoyl-sn-glycero-3-phosphoethanolamine-N-[biotinyl(polyethyleneglycol)-2000] (DSPE-PEG(2000)-Biotin) and 1,2-dipalmitoyl-sn-glycero-3-phosphoethanolamine-N-(7-nitro-2-1,3-benzoxadiazol-4-yl) (NBD). Xanthene erythrosin B, 3-aminopropyltriethoxysilane (APTES), streptavidin and neutrAvidin®-tetramethylrhodamine conjugate were purchased from Sigma-Aldrich. Glutaraldehyde (8%) was purchased from Polysciences. All chemicals were used without further purification

### Streptavidin-coated substrates

Glass coverslips (30 mm in diameter ) were: (i) cleaned with a piranha solution (75% of  $\text{H}_2\text{SO}_4$  and 25% of  $\text{H}_2\text{O}_2$ ), (ii) rinsed with milli-Q water, (iii) amino-functionalized by immersion in ethanol solution of 2% APTES for 5 minutes, (iv) heated at 110 °C in the oven for 15 minutes in order to stabilize the amino-silane layer, (v) incubated in a 4% glutaraldehyde solution for 1 hour and subsequently rinsed with milli-Q water, (vi) incubated for one hour in a saline phosphate buffer (PBS) solution containing 0.05 mg/mL of streptavidin and (vii) rinsed with PBS solution. This protocol was already described in<sup>1-2</sup>. For the purpose of evaluating the reliability of the above protocol, we initially imaged, using fluorescence microscopy, a streptavidin layer obtained by first mixing streptavidin and rhodamine modified neutravidin (ratio 1:1), prior to further incubation keeping the same procedure as above.

### **Buffer solutions and biotinylated GUVs electroformation.**

GUVs were prepared by the electroformation<sup>3</sup> method. Biotinylated DOPC and POPC GUVs were prepared by adding 2 mol % of DSPE-PEG(2000)-Biotin. Fluorescent GUVs were obtained by adding 0.5 mol % of NBD. Briefly, 10  $\mu\text{L}$  of a chloroform solution containing the lipid mixture (1 mg/ml) were spread on the surfaces of two conductive ITO (Indium Tin Oxide) glasses, which were then assembled with their conductive sides facing each other and separated by a 2-mm-thick Teflon frame, so to form a growing chamber. After drying under vacuum, the electroswelling chamber was filled with 200 mOsm  $\text{kg}^{-1}$  sucrose solution and connected to an alternating power generator at 1 V with a 10 Hz frequency for 2 h. Vesicles were then diluted 6 times in a 200 mOsm  $\text{kg}^{-1}$  PBS solution and dropped onto the streptavidin coated surfaces. The osmolarities of the sucrose and PBS solutions were measured with a cryoscopic osmometer Osmomat 030 (Gonotec, Berlin, Germany) and carefully matched to avoid osmotic pressure effects. The interplay between sucrose and PBS osmotically matches the inner and outer compartments of the vesicles and avoids their swelling and deswelling, especially under the strong adhesion conditions of the present study. An erythrosin-containing (1 mOsm  $\text{kg}^{-1}$ ) PBS solution was also prepared, with an osmotic pressure also adjusted to 200 mOsm  $\text{kg}^{-1}$ .

## **Observation and irradiation under an optical microscope**

Confocal microscopy images were taken for the purpose of illustration of the GUV adhesion (see Fig 1a in the paper); we used a TE2000 (Nikon, Japan) inverted microscope, equipped with a 100X oil-immersion objective, and a C1 confocal scanning head. Most of the present work, in particular GUV oxidation under irradiation and subsequent RICM observation of GUV adhesion, was performed under a TE200 inverted microscope (Nikon, Japan), equipped with a 100X oil immersion, a 40X DIC or a 40X phase contrast objectives. Images were acquired with a Diagnostic Instruments IN1800 digital camera and analyzed using a homemade software. Transmission (mainly DIC or phase contrast), fluorescence, and reflection interference contrast microscopy (RICM)<sup>4</sup> were used to image the GUVs. RICM allows to observe the GUV membrane in the vicinity of the substrate,<sup>4</sup> enabling in particular to follow the kinetics of adhesion of the biotinilated GUVs on the streptavidinated substrate (see Figure 1 and 2 in the paper). The RICM observation mode requires the association of a certain number of optical elements, i.e. a narrow band filtered illumination, a polarizer, an oil objective equipped with an outer quarter wave plate adapted to the observation wavelength, and an analyzer. In this study, we imaged the GUV adhesion using two illumination wavelengths, obtained using two narrow-band filters (Melles-Griot, bandwidth 10 nm): 436 nm ('blue') or 547 nm ('green'). The blue filter enabled RICM observation without vesicle perturbation, since erythrosin absorption around 436 nm is very small,<sup>5</sup> while the green filter was used for simultaneous RICM observation and photoactivation of erythrosin. In both wavelengths good enough interference images were obtained, enabling a precise measurement of the GUV adhesion patch dimensions, even though the quarter wave plate of our 100X objective was adapted for the green wavelength. The total

density power in the RICM mode at 547 nm, i.e. during oxidation, was ca.  $10 \text{ W/cm}^2$ , as measured previously.<sup>6</sup>

## Surface area increase

We consider a spherical vesicle with apparent radius  $R_0$ , i.e. of volume  $V_0 = \frac{4}{3}\pi R_0^3$ . Its apparent area  $S_0$  is related to  $R_0$  by  $S_0 = 4\pi R_0^2$ . We suppose that the vesicle is of real area  $S_{\text{real}} > S_0$  (some of the area is hidden in sub-optical thermal fluctuations). Let the vesicle adhere to a substrate, with preserved volume, so that its adhesion patch is round shaped with radius  $r$ , and the upper, non-adhered part is a spherical section of radius  $R$ . Then the volume  $V_0$  and the apparent surface  $S$  ( $S_0 < S \leq S_{\text{real}}$ ) of the adhered vesicle can be expressed as a function of  $R$  and  $r$ .

$$V_0 = \frac{2}{3}\pi R^3 \left( 1 + \frac{3}{2} \left( 1 - \frac{r^2}{R^2} \right)^{\frac{1}{2}} - \frac{1}{2} \left( 1 - \frac{r^2}{R^2} \right)^{\frac{3}{2}} \right) \quad (1)$$

$$S = \pi r^2 + 2\pi R^2 \left( \left( 1 - \frac{r^2}{R^2} \right)^{\frac{1}{2}} + 1 \right) \quad (2)$$

Expressing now all lengths in units of  $R_0$ , the radius  $R$  of a vesicle adhering under constant volume can be expressed as

$$R = \frac{1}{16} \left( \frac{r^8}{\Delta} + r^4 + \Delta \right) \quad (3)$$

with  $\Delta$  given by:

$$\Delta = \left( r^{12} + 128r^6 + 16 \left( \left( (r^6 + 16)(r^6 + 32) \right)^{\frac{1}{2}} + 128 \right) \right)^{\frac{1}{3}} \quad (4)$$

### Erythrosin addition effect

A stock solution of erythrosin was prepared, at  $1 \text{ mOsm kg}^{-1}$  concentration into a  $200 \text{ mOsm kg}^{-1}$  PBS buffer. A small volume, typically less than five microliters of this solution, was added at the end of stage ii (Figure 1.b) into the observation chamber containing the adhered biotinilated GUVs, so to reach the final concentration  $25 \mu\text{M}$  of erythrosin. We checked that this addition of erythrosin did not induce any modification of the GUV adhesion state. This was done following the evolution of the adhesion patch radius over minutes, in absence of ‘green’ irradiation. Figure S1 shows such typical evolution of ( $r$ ); only when the ‘green’ irradiation starts ( $P=10 \text{ W/cm}^2$ ,  $\lambda=547 \text{ nm}$ ) the adhesion patch undergoes an immediate and rapid increase, due to membrane area increase.

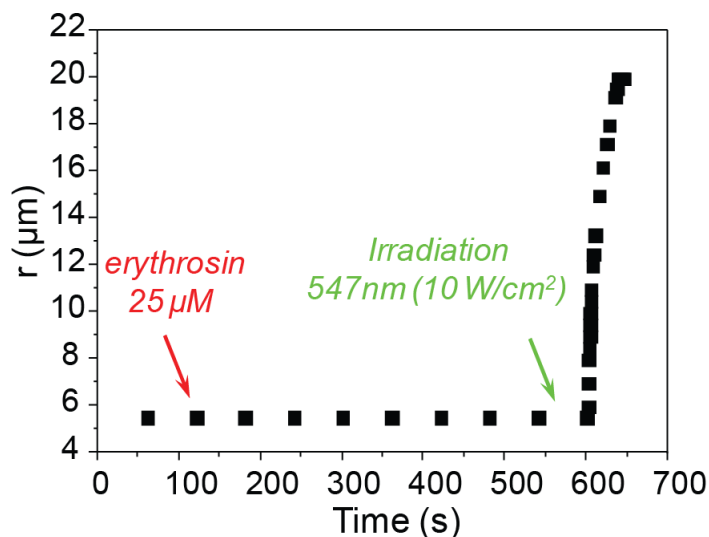


**Figure S1:** evolution of the adhesion patch radius ( $r$ ) of a biotinilated GUV after the addition of erythrosin in the surrounding medium (time of addition is shown by the red arrow). No effect is detected for minutes; only when ‘green’ irradiation starts (green arrow) the radius is seen to increase abruptly, corresponding to the membrane specific area increase, resulting from the hydroperoxidation of the lipid chain double bonds.

### **Start-stop experiments**

We performed start-stop experiments, submitting adhered biotinilated DOPC or POPC GUVs dispersed in an erythrosin-containing buffer (25  $\mu$ M of erythrosin) to successive ‘on-off’ irradiation stages, in order to see how membrane area increase correlates with light-induced oxidation. In practice, considering an adhered, stable GUV as that sketched on state (ii) in Figure 1.b, we first measure its internal volume from both the radius ( $r$ ) of its adhesion patch and from its equator radius ( $R$ ), using low power, ‘blue’, 435 nm light. Then, focusing on the substrate plane so to get an interference RICM image of the adhesion patch, we submit the GUV to successive ‘on-off’ irradiation steps, under continuous imaging, corresponding to successive switching from ‘blue’ light to ‘green’, 547 nm, high power irradiation. The membrane adhesion patch can be continuously imaged, provided that the camera gain and/or exposure time are manually changed with irradiation wavelength, which takes less than one second. The evolution with time of the relative surface area increase is given in Figure S2 for a typical experiment. It can be seen that there is no delayed effect when starting or stopping the irradiation. When the surface area reaches its maximum value, the GUV is imaged in blue and its volume is again measured so to check if the whole process was achieved at constant volume. This test proves the correlation existing between sensitizer excitation and membrane lipid double bond(s) hydroperoxydation.

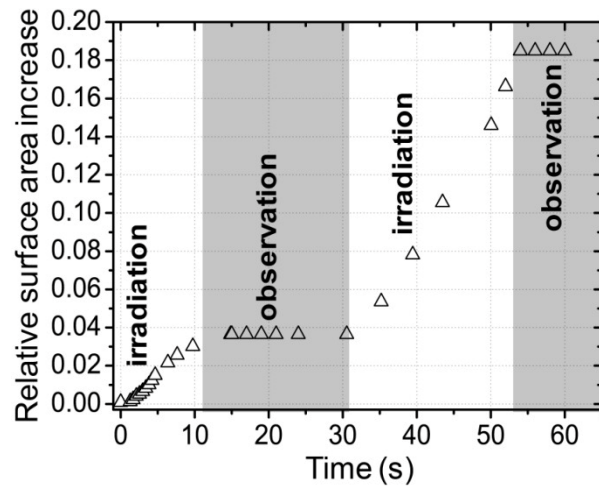


**Figure S2:** relative surface area increase as a function of time, alternating irradiation ('green', full power) and observation ('blue'), for an adhered biotinylated DOPC GUV into a buffer solution containing 25  $\mu\text{M}$  of erythrosin.

## Leakage

It was crucial to verify that the membrane area increase with oxidation, that is revealed by the increase of the GUV adhesion patch size, is a process that takes place without any leakage of the vesicle internal solution. For that purpose the following protocol has been applied for each studied GUV: at the end of the first adhesion stage (sketched by ii in Figure 1.b), we systematically measured both the adhesion patch radius  $r_1$  and the equator radius  $R_1$  (from RICM and fluorescence respectively), that allowed us to calculate the GUV internal volume ( $V_1$ ). The erythrosin was then added into the solution, and after circa. one minute the irradiation was started ('green', high power illumination) while continuous image acquisition was performed. Once the adhesion patch reached a new, stable value, the irradiation was stopped and the adhesion patch and equator radii  $r_2$  and  $R_2$  were measured, and the internal volume ( $V_2$ ) calculated. Only if  $V_1$  and  $V_2$  were identical within the experimental error the GUV was validated and its increase in membrane area calculated. Figure S3 presents the  $V_2/V_1$  values for all DOPC and POPC selected vesicles; one gets  $V_2/V_1 = 1.00$  with less than 2% error. Only very few GUVs experienced bursting or leakage during oxidation (less than 5%). There is little to say about GUV bursting: this may be due to any membrane defect and is of low interest here. Bursting GUVs are obviously not taken into account. Concerning the GUVs that undergo leakage ( $V_2/V_1 < 1$ ) with oxidation, the fact that they represent a small fraction of the whole (<5% only) is certainly due to some specific property of oxidized DOPC and POPC. The bilayer internal cohesion force remains strong enough, i.e. higher than the tension generated by the biotin-streptavidine adhesion energy. The important point here is that these vesicles show a relatively high level of leakage (when they do leak), typically  $V_2/V_1 < 0.5$ . This is certainly due to the high tension of the bilayer imposed by the present adhesion conditions; indeed the biotin-streptavidin bond has one of the highest binding energy in the bio-world. Thus, the leakage appears clearly

from the measure of the adhesion patch radius. There is in fact no need to check the final GUV volume  $V_2$ ; following simply the adhesion radius evolution with time is enough to guess that the GUV underwent leakage.

Finally, the fact that DOPC and POPC GUVs rarely leak during oxidation leads us to believe that the initial, non oxidized GUVs that are left to sediment and adhere on the streptavidinated bottom surface, reaching stage (ii) on Figure 1.b, should identically reach this stable, stretched state with smeared thermal fluctuations without having sustained any leakage.

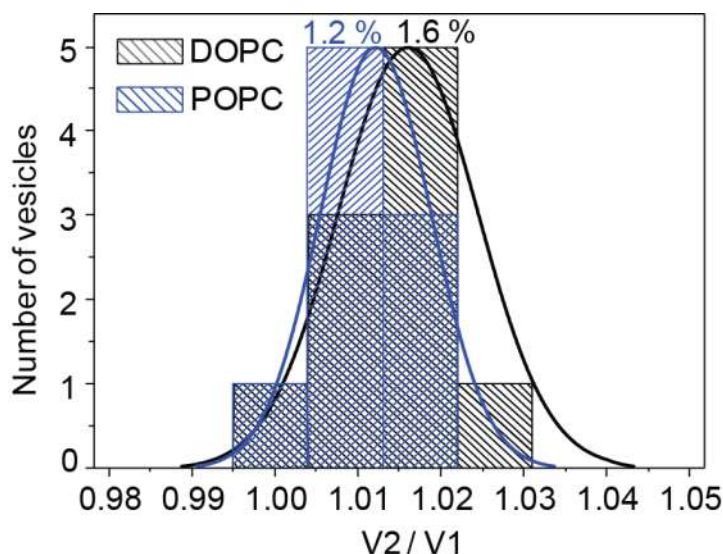


**Figure S3:** distribution of the  $V_2/V_1$  values for all DOPC and POPC studied GUVs.  $V_1$  is the volume before and  $V_2$  after oxidation.  $V_1$  and  $V_2$  are calculated from  $r$  and  $R$ , using the formula of the volume of a truncated sphere.

## Loss of contrast

The contrast in the RICM image of a stable, oxidized membrane appears lower than the contrast of the initial patch, i.e. before oxidation started, as shown in Figure 1. In fact, the lowering of the contrast was seen to start at various moments of the oxidation process, depending on the vesicle, but always after several tens of seconds of irradiation. Two examples are given in the following Figure S4; it can be seen that the loss of contrast may follow the stabilization of the area increase (left), or start before it (right). However, in both situations depicted by Figure S4, the area increase remains unmodified by the gray level variation: in the case of a membrane area still on its increasing stage when the contrast starts to decrease, no modification of the area rate of increase is observed (right); if the area already reached its stable final value before the gray level starts to decrease, no modification of the area is observed (left). Again, membrane area is here calculated from geometrical values of  $r$  (i.e. in real time from RICM) but with a systematic measure of the equator radius  $R$  at the end of the process, in order to control that the internal volume of the GUV remained constant through the overall process (see above). We argue that it's not reasonable to invoke some leakage (with sucrose/glucose exchange) while the adhered membrane keeps its internal volume. Any pore opening followed by leakage is not compatible with volume conservation, since the membrane is under some strong tension due to the adhesion. Understanding this gray level decrease is also beyond the scope of this article, but we can invoke at least three mechanisms: i) an increase of the membrane-substrate distance, due to strong modification of the membrane-substrate interactions (we should remind that an important fraction of the membrane surface should be populated with -OOH groups at the end of the hydroperoxidation process); ii) the lateral membrane area increase of 15-19% might also contribute to a change in the membrane substrate distance in the patch region, because of some

geometrical hindrance that reduces lateral diffusion of lipids out of the adhesion patch, due to the high concentration of biotin-streptavidin links; and iii) the membrane should also be thinner by a factor of circa 8% since its surface area increases by 14-19%. Other reasons might also be at the origin of that loss of contrast, but our experiments clearly show no leakage, as demonstrated by Figure S3.

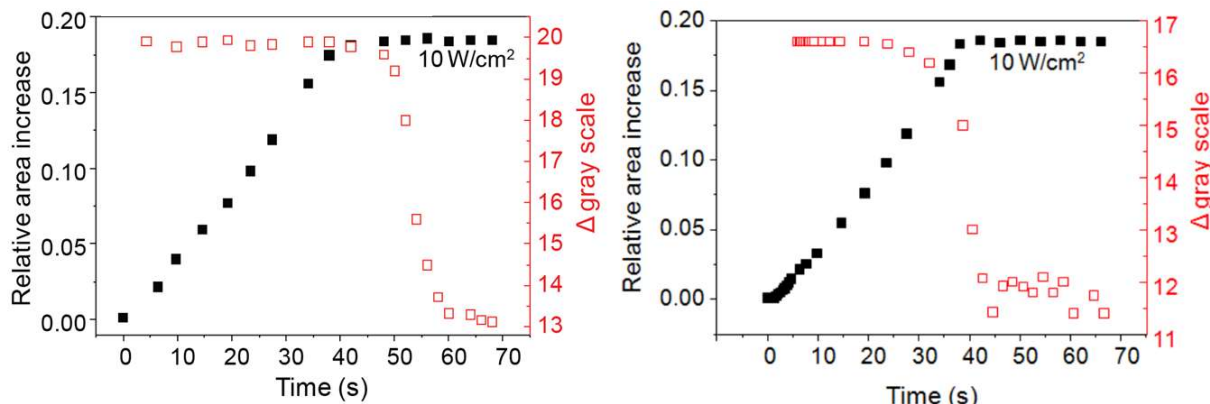


**Figure S4:** time evolution of membrane area (as measured from  $r$ , the adhesion patch radius) and contrast between the inside and outside of the adhesion patch, for two DOPC vesicles. For each vesicle we measure  $V_2$  from  $r_2$  and  $R_2$ , and check that  $V_2=V_1$  within the experimental error (see Figure S3).

Finally, for a matter of illustration, Figure S5 shows a typical evolution of the adhesion patch under continuous irradiation. Figures S5a and S5b correspond to the starting point and the ending point of area increase, respectively. Only 90 seconds later, while illumination still goes on, one can observe the dramatic effect of the membrane rupture that is highlighted by the presence of some inhomogeneous membrane repartition on the substrate. Besides, one could wonder why on Figure S5c the original adhesion patch (the one created prior to oxidation process) is preserved, while the part of the patch that was generated during oxidation appears strongly modified after the membrane rupture. One can deduce from these observations that not only the mechanism of oxidation is complex, modifying strongly both the membrane properties and the interactions of the membrane with our streptavidinated substrate, but also the adhesion geometry used to reveal

lipid area increase is itself complex, with a finite number of ligands on the membrane, a finite diffusion coefficient of these ligands, amongst others, all these factors contributing possibly to the observed inhomogeneities and contrast variations as seen in RICM. However, we undoubtedly were able to reveal and measure the lipid area increase due to oxidation, from the round-shaped adhesion patches measured at stages II and III, which correspond to stable states.

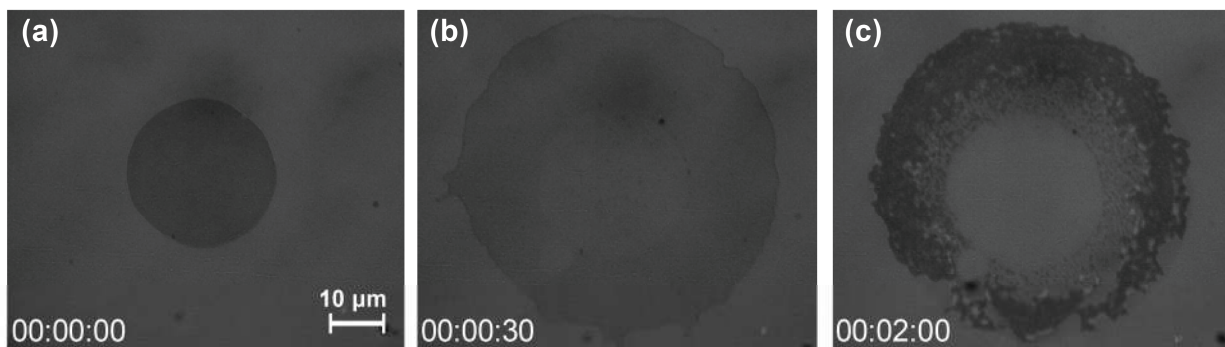


**Figure S5:** RICM evolution of the adhesion patch (a) before, (b) after irradiation and (c) after vesicle collapse.

### ***Strong adhesion, membrane tension, GUV shape***

We calculate the volume of our adhered GUVs assuming that their shape is that of a truncated sphere. Checking this point with confocal microscopy is easy but the same information can be obtained using other arguments, as obtained from the literature. For that we need first to evaluate the membrane tension of the adhered GUVs. For that we refer to the seminal paper of E. Evans,<sup>7</sup> that relates the contact angle, the tension and the adhesion energy between the membrane and the substrate, comparing the limit situation defined by a high density of linkers to the case of a low density of linkers. In the present study, we argue that we are close to the limit defined as that of a ‘high density of linkers’. Indeed, the vesicles adhere on a glass that is functionalized with a monolayer of streptavidin molecules, the area of which is circa  $25 \text{ nm}^2$ . The biotin molar fraction in the membrane is 2%, corresponding to an area concentration of circa one biotin per  $33 \text{ nm}^2$  (considering a lipid area of  $65 \text{ \AA}^2$ ). Thus, the area concentrations of ligands and receptors match approximately, a condition that we imposed so to optimize the adhesion force and efficiency. According to,<sup>7</sup> of importance for the calculation of the membrane tension is the ratio  $l_g/l_b$ , of the distance between two neighboring links in the adhesion patch, to the characteristic distance of the adhesion interaction. Here  $l_g$  is of the order of 5 nm, while  $l_b$  is of the order of 10 nm (i.e. a fraction of the PEO contour length, the carbon spacer that links the biotin head to the lipid head);  $l_g/l_b$  is therefore of the order of, or even smaller than one. In this case, according to,<sup>7</sup> the Youngs equation  $T=W(1-\cos \theta)$  is valid and enables to calculate the membrane tension knowing  $W$ , the adhesion energy, and  $\theta$ , the membrane-substrate contact angle. First,  $W$  can be calculated easily:  $W=w \cdot f$ , and  $f$  is the surface area concentration of links in the adhesion patch, and  $w=40 \text{ k}_B T$  is the typical binding energy of a biotin-streptavidin bond; thus  $W=5 \text{ mN/m}$  considering one link per  $30 \text{ nm}^2$ . Furthermore, from our RICM images one can determine that  $\theta$  is always higher than

60°, since no interference ring is visible around the adhesion patch. This leads to a value for the membrane tension of circa  $T=2.5$  mN/m (taking  $\theta=60^\circ$ ). This value is an overestimation since we consider that almost 100% of the streptavidins covering the substrate are linked to a biotin of the membrane in the adhesion patch region. However, even for a five times smaller value, could we still consider that the membrane tension is high enough so to smear out the membrane thermal fluctuations. Indeed, experimental studies of GUV deformation under suction, using a micropipette device, have clearly shown that for tensions higher than 0.5-1.0 mN/m membrane thermal fluctuations can be considered as smeared out, see for example.<sup>8</sup> So we argue that in our adhesion conditions, our vesicles can indeed be considered as being tensed enough so that no significant thermal fluctuations remain. Any measured increase of membrane surface area is therefore a real increase of the specific membrane area, and not a simple smearing out of some non visible, excess of membrane that would be stored under the form of thermal fluctuations.

A second argument is now necessary to establish that the shape of our adhered GUVs is that of a truncated sphere. It is known that the bending energy of the membrane fights against the establishment of the contact angle in the vicinity of the substrate surface. For papers treating this situation, one can cite.<sup>9</sup> The effect of a finite bending modulus is that, out of the adhesion patch, the membrane becomes a spherical cap only after a distance  $\lambda$  from the patch border, with  $\lambda=(\kappa/\sigma)^{1/2}$ ,  $\kappa$  is the bending rigidity and  $\sigma$  is the membrane tension. Taking  $\kappa=20$   $k_B T$  and  $\sigma=0.2$  mN/m reads  $\lambda=20$  nm, a very small distance compared to the overall dimension of the GUV. Therefore, the deviation from the pure truncated sphere can be ignored in the present case.

## References

1. R. Lehner, J. Koota, G. Maret and T. Gisler, *Physical Review Letters*, 2006, **96**.
2. Y. T. L. Sun, N. K. Mani, D. Baigl, T. Gisler, A. P. Schroder and C. M. Marques, *Soft Matter*, 2011, **7**, 5578-5584.
3. M. I. Angelova and D. S. Dimitrov, *Faraday Discussions*, 1986, **81**, 303-311.
4. J. Radler and E. Sackmann, *Journal De Physique Ii*, 1993, **3**, 727-748.
5. D. S. Pellosi, B. M. Estevao, J. Semensato, D. Severino, M. S. Baptista, M. J. Politi, N. Hioka and W. Caetano, *Journal of Photochemistry and Photobiology a-Chemistry*, 2012, **247**, 8-15.
6. W. Caetano, P. S. Haddad, R. Itri, D. Severino, V. C. Vieira, M. S. Baptista, A. P. Schroder and C. M. Marques, *Langmuir*, 2007, **23**, 1307-1314.
7. E. A. Evans, *Biophysical Journal*, 1985, **48**, 185-192.
8. E. Evans and W. Rawicz, *Physical Review Letters*, 1990, **64**, 2094-2097.
9. U. Seifert and R. Lipowsky, *Physical Review A*, 1990, **42**, 4768-4771.